

Modelling the Excitation of Guided Waves in Generally Anisotropic Multi-layered Media

Alexander VELICHKO, Paul WILCOX, Department of Mechanical Engineering, University of Bristol, United Kingdom

Abstract. Guided acoustic waves are an attractive basis for rapid non-destructive evaluation (NDE) and global structural health monitoring (SHM) due to their relatively long propagation distances and sensitivity to defects. The design of transducers to excite and detect guided waves is a fundamental part of an NDE or SHM system and requires the ability to predict the radiated guided wave field of a transmitting transducer. For most transducers, this can be performed by making the assumption that the transducer is weakly coupled and then integrating the Green's function of the structure over the area of the transducer. The majority of guided wave modelling is based on two-dimensional (2D) formulations where plane, straight-crested waves are modelled. Several techniques can be readily applied to obtain the solution to the forced 2D problem in terms of modal amplitudes. However, for transducer modelling it is desirable to obtain the complete three-dimensional (3D) field, which is particularly challenging in anisotropic materials. In this paper, a technique for obtaining a far-field asymptotic solution to the 3D Green's function in terms of the modal solutions to the forced 2D problem is presented. Results are shown that illustrate the application of the technique to isotropic and anisotropic plates. Where possible, results from the asymptotic model are compared to those from 3D time-marching finite element simulations and good agreement is demonstrated.

Introduction

The analysis of guided waves in multi-layered media has been the subject of a considerable amount of research for over a century. The first solutions of the unforced modal problem considered a two-dimensional (2D) cross section through the waveguide. In this formulation, the media are assumed to be in a state of plane-strain and the guided wave modes predicted are plane, straight-crested waves with wavefronts perpendicular to the cross section. In the current paper, the plane-strain formulation for straight-crested guided waves is referred to as the 2D formulation. Much research has been devoted to analysing the dispersion relationships for guided waves using the 2D formulation and a number of methods of solution have been developed including global and transfer matrix methods [1] and semi-analytical finite element (SAFE) methods [2]. Numerical solutions using some of these methods are well established and commercially available [3]. Although less well known, the tools for predicting the amplitude of excited guided waves based on a 2D formulation are also well established. For example the forced problem can be solved directly by using integral transforms [4], the SAFE method [5] or by using modal expansion and the principle of reciprocity [6].

In practice the modal solution obtained from a 2D formulation provides an adequate basis for understanding many aspect of wave propagation in real three-dimensional (3D) structures. However the 2D formulation is a much less satisfactory basis for modelling the radiated guided wave field from a finite sized transducer, since the 2D formulation

inherently requires the force distribution to extend infinitely in the plane perpendicular to the cross section. To accurately model a transducer a 3D formulation is required. There are several approaches to finding the solution of the 3D forced problem. For example, the 3D wave field due to surface load can be calculated by using multiple integral transforms coupled with matrix methods for isotropic [7] and anisotropic [8] materials or using a modal expansion method [9]. It is also possible to use the finite element method [10] or other numerical methods [11].

In this paper, the 3D Green's function is written in such a way that its far field asymptotic solution can be expressed in terms of the modal expansion of a forced 2D system, which, as previously noted, can be obtained by a number of established methods. A technique is therefore provided for numerically computing the 3D excited guided wave field from a finite sized transducer using only the dispersion relationships and mode shapes obtained from 2D formulations. The technique is applicable to generally anisotropic layered media, although the relationship between 2D and 3D solutions is more complex than in isotropic or transversely isotropic layered media.

1. Formulation of General 3D Problem

A planar multi-layered system consisting of N generally anisotropic layers is considered with Cartesian coordinate axes (x, y, z) defined with the z axis normal to the plane of the layers. An arbitrary time harmonic load $\mathbf{q}^{(3)} e^{-i\omega t}$ is applied to the upper surface of the system $z=0$. The resulting time-harmonic displacement field in the system due to $\mathbf{q}^{(3)}$ is denoted by $\mathbf{u}^{(3)}$. The function $\mathbf{u}^{(3)}$ is related to $\mathbf{q}^{(3)}$ by the 3D Green's function $\mathbf{g}^{(3)}(x, y, z)$:

$$\mathbf{u}^{(3)}(x, y, z, \mathbf{q}^{(3)}) = \iint \mathbf{g}^{(3)}(x - x', y - y', z) \mathbf{q}^{(3)}(x', y') dx' dy' \quad (1)$$

The Green's function, $\mathbf{g}^{(3)}$, can be written in terms of its 2D spatial Fourier transform, $\mathbf{G}^{(3)}$, as

$$\mathbf{g}^{(3)}(x, y, z) = \frac{1}{4\pi^2} \iint \mathbf{G}^{(3)}(k_x, k_y, z) e^{i(k_x x + k_y y)} dk_x dk_y \quad (2)$$

where the matrix $\mathbf{G}^{(3)}(k_x, k_y, z)$ is the Green's function for straight-crested waves propagating in the direction given by the components k_x, k_y of the wave vector.

2. 2D Problem

A new coordinate system (ξ, η, z) is defined that is a rotation of the original coordinate system by an angle γ . A special case of $\mathbf{q}^{(3)}$ may be defined as $\mathbf{q}^{(2)}(\xi)$ which is invariant in the ξ direction. The displacement field due to this loading is defined as $\mathbf{u}^{(2)}(\gamma, \xi, z, \mathbf{q}^{(2)})$. The loading $\mathbf{q}^{(2)}$ and displacement $\mathbf{u}^{(2)}$ represent the case of 2D excitation. The relationship between $\mathbf{u}^{(2)}$ and $\mathbf{q}^{(2)}$ may be written as the convolution integral

$$\mathbf{u}^{(2)}(\gamma, \xi, z, \mathbf{q}^{(2)}) = \int \mathbf{g}^{(2)}(\gamma, \xi - \xi', z) \mathbf{q}^{(2)}(\xi') d\xi' \quad (3)$$

where $\mathbf{g}^{(2)}$ is the 2D Green's function. $\mathbf{g}^{(2)}$ can be written in terms of its 1D spatial Fourier transform, $\mathbf{G}^{(2)}$, as

$$\mathbf{g}^{(2)}(\gamma, \xi, z) = \frac{1}{2\pi} \int \mathbf{G}^{(2)}(\gamma, k, z) e^{ik\xi} dk \quad (4)$$

By using the residues technique, the integration in (4) can be reduced to the sum of residuals:

$$\mathbf{g}^{(2)}(\gamma, \xi, z) = \sum_m \mathbf{E}_m^{(2)}(\gamma, z) e^{ik_m \xi}, \quad \mathbf{E}_m^{(2)}(\gamma, z) = i \operatorname{res} \mathbf{G}^{(2)}(\gamma, k, z) \Big|_{k=k_m} \quad (5)$$

where $\mathbf{E}_m^{(2)}$ is defined as the 2D modal excitability matrix.

The real poles represent the propagating waves while the complex poles represent nonpropagating waves that decay exponentially with propagation distance from the source. In this paper only the contributions from real poles are considered.

To solve the 2D problem using the described integral transforms method it is necessary to calculate matrix $\mathbf{G}^{(2)}$. The modal solution of the forced 2D problem can also be obtained by a number of other established methods. For example, the reciprocity approach [6] leads to an alternative expression for mode amplitude $\mathbf{E}_m^{(2)}$ that is useful because it can be computed directly from the mode shape.

3. Relation between 2D and 3D Problems for Straight-crested Waves

Consider now the relationship between 2D and 3D Green's functions for straight-crested waves $\mathbf{G}^{(2)}$ and $\mathbf{G}^{(3)}$. The transformation from the coordinate system (x, y, z) to the new coordinate system (ξ, η, z) is represented by the matrix \mathbf{A} :

$$\begin{pmatrix} \xi \\ \eta \\ z \end{pmatrix} = \mathbf{A}(\gamma) \begin{pmatrix} x \\ y \\ z \end{pmatrix}, \quad \mathbf{A}(\gamma) = \begin{pmatrix} \cos \gamma & \sin \gamma & 0 \\ -\sin \gamma & \cos \gamma & 0 \\ 0 & 0 & 1 \end{pmatrix} \quad (6)$$

The Green's matrix in the Fourier domain, $\mathbf{G}^{(3)}(k_x, k_y, z)$, is transformed as:

$$\mathbf{G}_\gamma^{(3)}(k_\xi, k_\eta, z) = \mathbf{A} \mathbf{G}^{(3)}(k_\xi \cos \gamma - k_\eta \sin \gamma, k_\xi \sin \gamma + k_\eta \cos \gamma, z) \mathbf{A}^{-1} \quad (7)$$

Here $\mathbf{G}_\gamma^{(3)}(k_\xi, k_\eta, z)$ is the Green's function for straight-crested wave with wave vector $(k_\xi, k_\eta, 0)$. On the other hand, $\mathbf{G}^{(2)}(\gamma, k, z)$ is Green's function for straight-crested wave with wave vector $(k, 0, 0)$. Hence,

$$\mathbf{G}^{(2)}(\gamma, k, z) = \mathbf{A} \mathbf{G}^{(3)}(k \cos \gamma, k \sin \gamma, z) \mathbf{A}^{-1} \quad (8)$$

4. Far-field Asymptotic Solution to 3D Problem

Expression (5) gives the expansion of the 2D solution in terms of 2D modes. In this section the analogous mode expansion of the 3D solution in the far-field will be derived. As in the 2D case the mode amplitudes are proportional to the residuals for real poles of the matrix $\mathbf{G}^{(3)}$. Then by using (8) it is possible to obtain the relationship between mode amplitudes in 2D and 3D cases.

First a change of global coordinates from Cartesian (x, y, z) to cylindrical polar (r, φ, z) is defined: $x = r \cos \varphi, y = r \sin \varphi, k_x = k \cos \gamma, k_y = k \sin \gamma$. The expression (2) for the 3D Green's function $\mathbf{g}^{(3)}$ can therefore be written in polar coordinates as:

$$\mathbf{g}^{(3)}(r, \varphi, z) = \frac{1}{4\pi^2} \int_{\varphi-\pi/2}^{\varphi+3\pi/2} \left\{ \int_{\Gamma} \mathbf{G}^{(3)}(k \cos \gamma, k \sin \gamma, z) e^{ikr \cos(\gamma-\varphi)} k dk \right\} d\gamma \quad (9)$$

The contour of integration Γ coincides with the real positive half-axis except for real poles. In these points it diverges in the complex plane k in accordance with the principle of limiting absorption [7].

The integration with respect to k can be performed by using the residues theory. Then Integral with respect to γ is then calculated using the stationary phase method. This enables the expression for the far field asymptote to the 3D problem to be written as:

$$\mathbf{g}^{(3)}(r, \varphi, z) = \frac{1}{\sqrt{r}} \sum_m \mathbf{E}_m^{(3)}(\varphi, z) e^{ir\Phi_m(\gamma_m, \varphi)} + O(r^{-3/2}), \quad r \rightarrow \infty \quad (10)$$

$$\mathbf{E}_m^{(3)}(\varphi, z) = i B_m(\varphi) \operatorname{res} \mathbf{G}^{(3)}(k \cos \gamma_m, k \sin \gamma_m, z) \Big|_{k=k_m}, \quad k_m = k_m(\gamma_m)$$

where $\mathbf{E}_m^{(3)}$ is defined as the 3D modal excitability matrix.

The phase functions Φ_m and coefficients B_m are given by:

$$\begin{aligned} \Phi_m(\gamma, \varphi) &= k_m(\gamma) \cos(\gamma - \varphi), \\ B_m &= \frac{|k_m(\gamma_m)|}{\sqrt{2\pi|b_m|}} \exp(i \frac{\pi}{4} \operatorname{sgn} b_m), \quad b_m = \frac{d^2 \Phi(\gamma_m)}{d\gamma^2} \end{aligned} \quad (11)$$

The angle $\gamma_m \equiv \gamma_m(\varphi)$ is found from the following equation

$$\varphi = \gamma_m + \arctan\left(\frac{1}{c(\gamma_m)} \frac{dc(\gamma_m)}{d\gamma}\right) \quad (12)$$

here $c(\gamma) = \omega/k(\gamma)$ is phase velocity.

5. Relation between 2D and 3D Problems

In summary, the 2D Green's function is:

$$\mathbf{g}^{(2)}(\gamma, \xi, z) = \sum_m \mathbf{E}_m^{(2)}(\gamma, z) e^{ik_m \xi}$$

and the far-field asymptotic to the 3D Green's function is:

$$\mathbf{g}^{(3)}(r, \varphi, z) = \frac{1}{\sqrt{r}} \sum_m \mathbf{E}_m^{(3)}(\varphi, z) e^{ir\Phi_m(\gamma_m, \varphi)}.$$

Using expression (8), the modal excitability matrices in the 2D and 3D cases can be related by:

$$\mathbf{E}_m^{(3)}(\varphi) = B_m(\varphi) \mathbf{A}^{-1}(\gamma_m) \mathbf{E}_m^{(2)}(\gamma_m) \mathbf{A}(\gamma_m) \quad (13)$$

The far field solution for a particular mode in the φ direction is therefore intimately related to the appropriate 2D solution for the same mode in the γ_m direction. The angle(s) γ_m is the phase velocity direction(s) for the m^{th} mode with group velocity in the φ direction.

It is supposed in the previous analysis that $b_m \neq 0$. It can be shown that if $b_m = 0$ then $d\varphi/d\gamma = 0$. In this case the group velocity direction remains the same while the phase velocity direction varies and in such directions the wave field decays as $O(r^{-1/3})$.

The complete procedure for predicting the far field displacement in the φ direction under point harmonic loading is as follows:

- Compute dispersion relationships $k_m(\gamma)$. For m^{th} mode, find angle or angles γ_m .
- Solve 2D problem at angle γ_m .
- Compute the amplitude of 3D mode at angle φ from 2D solution at angle γ_m .

6. Implementation of asymptotic model

The analytic model described in the previous section has been implemented numerically using functions written in the Matlab (The Mathworks Inc., Natick, Massachusetts) modelling environment and can be separated into two distinct parts. The first part of the program generates dispersion data for the structure and the second part converts this into modal excitability matrices for guided wave propagation in a specified direction.

Dispersion curves are generated for different angles of propagation using a semi-analytic finite element technique (implemented in Matlab) similar to that described by Hayashi, etc [2]. For each angle, γ , this technique yields a number of discrete points lying in $\omega - k$ space, where k is complex. Each point corresponds to a modal solution for the propagation of straight-crested guided waves in the γ direction.

The most challenging aspect of the numerical implementation is to link the discrete points in $\omega - k - \gamma$ space together into modes to create dispersion surfaces. First, points are linked at each γ angle by comparing the mode shapes at nearby points in $\omega - k$ space to form dispersion curves. Next, dispersion curves are linked between adjacent γ angles to form dispersion surfaces by comparing both mode shapes and dispersion curve shapes.

Once the dispersion data is obtained for all modes excitability matrices for any mode, m , frequency, ω_0 , and propagation direction, φ , can be computed. The 2D excitability matrix is calculated by using the reciprocity approach [6]. The 3D excitability matrix is computed according to (13) and the effective wavenumber in the φ direction, Φ_m , is calculated from (11).

The excitability matrix and effective wavenumber provide all information necessary to perform wave excitation simulation. Typically this may involve the simulation of either time-domain signals recorded at a particular point or the surface displacement around a source at a particular instant in time.

7. Finite Element Modelling

In order to validate the implementation of the three-dimensional (3D) excitability model described in the previous sections, a number of 3D explicit time marching finite element (FE) simulations have been performed. The maximum size of FE model that can be run on the computer resources available is limited to around 5×10^6 degrees of freedom and this means that a compromise must be made between the size of structure modelled and the mesh density. For this reason, the mesh density used is somewhat less than ideal and this is manifested in an underestimate of guided wave velocity that is more pronounced for short wavelength modes. Notwithstanding these limitations, the FE results are sufficient to qualitatively show that the excitability algorithm has been correctly implemented and also to indicate the regions where the asymptotic assumptions break down.

The general FE model geometry, used here, is shown in Fig.1. All FE modelling was performed using the ABAQUS package (Version 6.5.2, ABAQUS Inc., Providence, RI, USA) running on a Viglen CL2000, using a single Intel Xeon 32 GHz processor incorporating 64-bit PCI with a Linux operating system and 8GB RAM.

For comparison purposes, the displacement field due to each mode should ideally be analysed separately. However, while the analytic model can be used on a mode by mode basis, the FE model implicitly includes the contributions from all guided wave modes. A rudimentary method for partially separating the contributions from different modes in the FE model, which has been employed here, is to monitor displacements at nodes on both upper and lower surfaces of the plate. This then allows the contributions to be separated into those due to symmetric and anti-symmetric nodes. In the relatively low frequency thickness regime where the modelling has been performed in this paper only three fundamental mode types exist corresponding to A_0 and S_0 Lamb type modes and a symmetric SH type mode, referred to as SH_0 . The modal separation technique employed therefore allows complete separation of the A_0 mode but not of the S_0 and SH_0 modes.

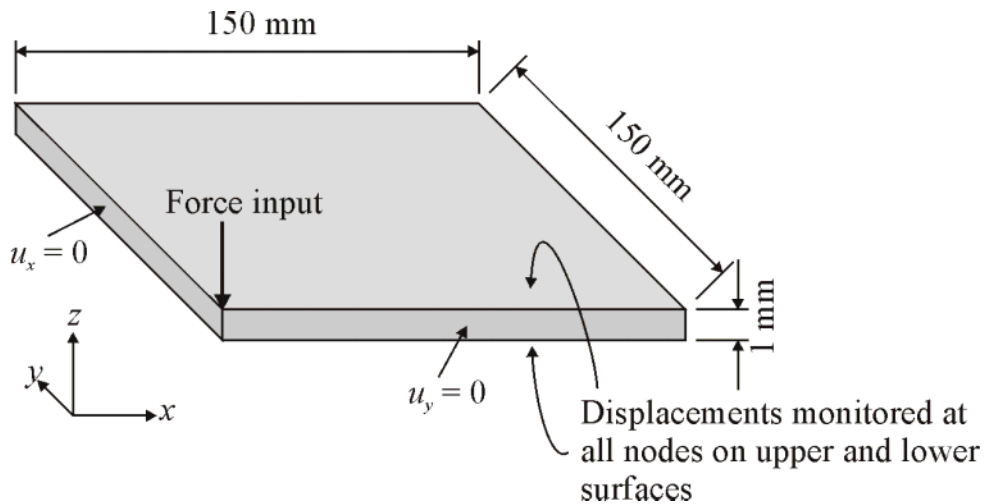


Fig.1. Finite element (FE) model geometry.

8. Results

The excitation of guided waves by an out-of-plane point force in an isotropic plate and highly anisotropic plate are presented here to illustrate the capability and limitations of the asymptotic model. In all cases, a 1 mm thick plate is considered and the excitation signal is a 5 cycle Hanning windowed toneburst with a centre frequency of 300 kHz.

8.1. Out-of-plane Excitability of Isotropic Plate

The first case considered is an isotropic aluminium plate (density is 2700 kg m^{-3} , Young's modulus is 70 MN mm^{-2} and Poisson's ratio is 0.3). A_0 , S_0 and SH_0 modes may exist in this system. However, the isotropy of the plate and orientation of the input force means that the problem is axi-symmetric and hence only A_0 and S_0 are excited. Figs. 2(a) and 2(b) show snapshots of the out-of-plane surface displacement $25 \mu\text{s}$ after the start of the input signal obtained from the FE model for the A_0 and S_0 modes. The non-axi-symmetric signal near the origin in Fig.2(b) is due to the unwanted presence of higher order modes at the upper frequency limit of the input signal that cannot be correctly modelled by the mesh density used. Fig.2(c) and 2(d) show the equivalent results obtained from the asymptotic analytic model. The grey scale in both images is the same, and it can be seen that the FE and analytic models are in excellent agreement.

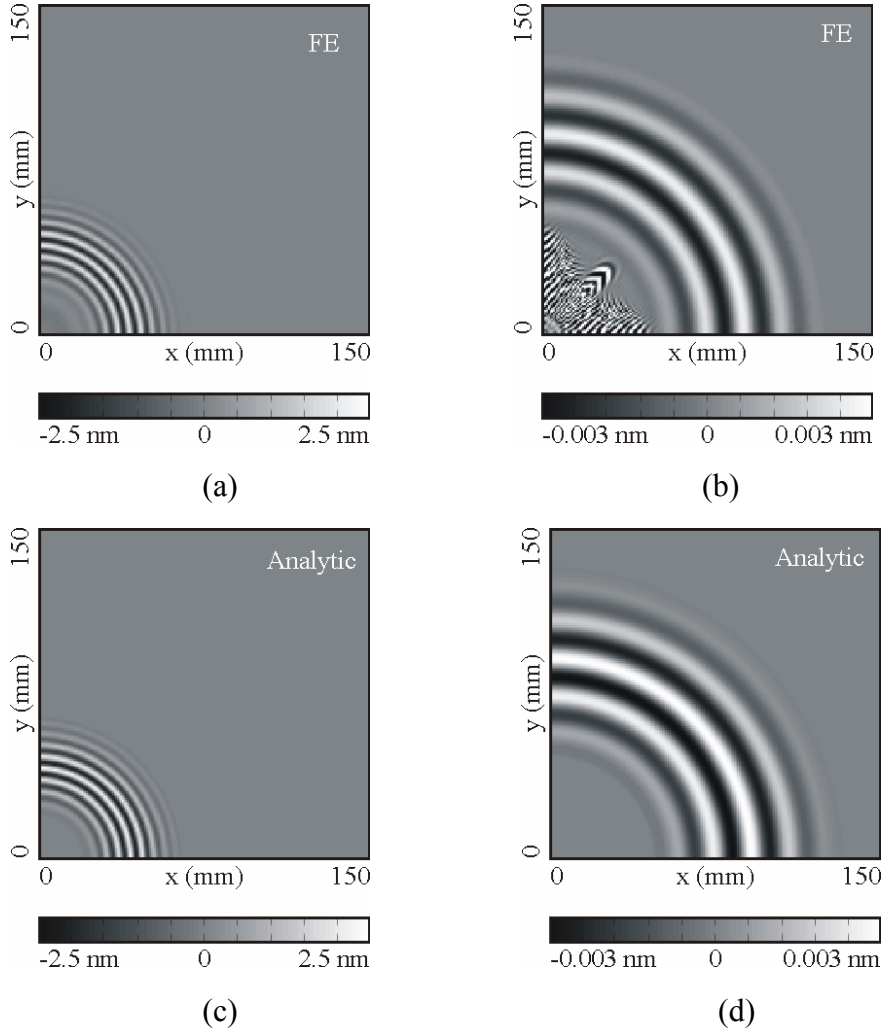


Fig.2. Out-of-plane surface displacement of an aluminium plate: FE model results showing contributions from (a) A_0 mode and (b) S_0 mode; analytic model results showing contributions from (c) A_0 mode and (d) S_0 mode.

8.2. Cross-ply Composite Plate

A cross-ply composite plate has been modelled using equivalent homogenous properties which are listed in Table 1. Again over the frequency range considered A_0 , S_0 and SH_0 type modes may exist in this system. However it should be noted that, other than in the 0° and 90° directions the mode shapes of S_0 and SH_0 both contain displacement components in directions parallel and perpendicular to the direction of propagation, hence the designation of the mode names in these directions is ambiguous. However, this attribute of the mode shapes means that in this system, all three modes are excited by the application of an out-of-plane point force in certain directions.

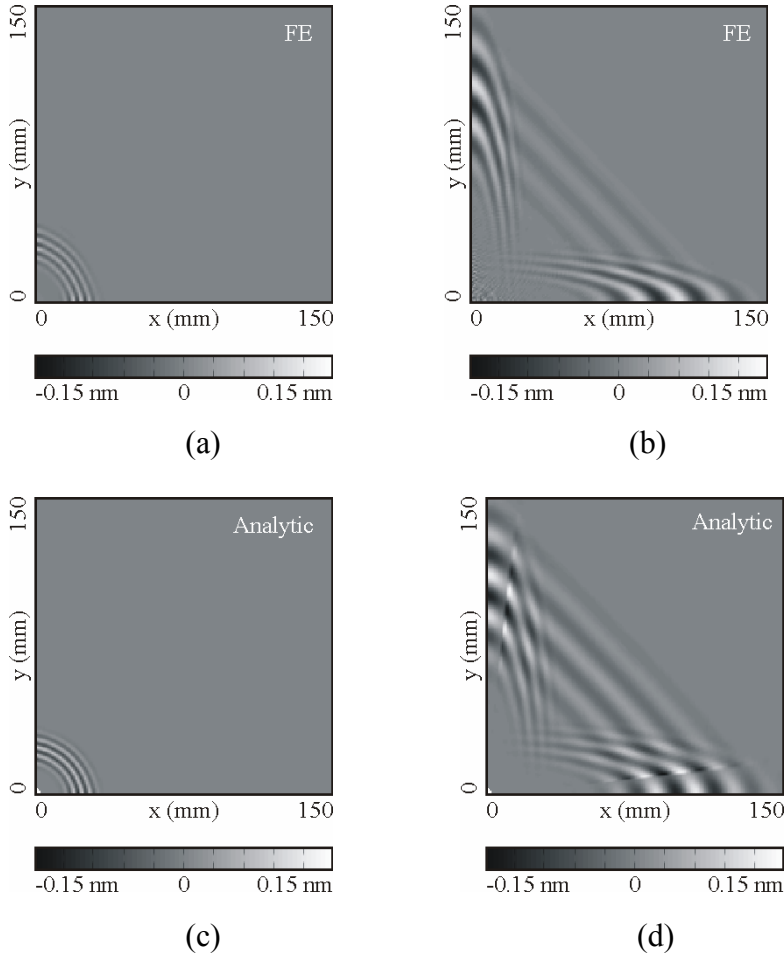
Figs.3(a) and 3(b) show snapshots of the out-of-plane surface displacement 25 μ s after the start of the input signal obtained from the FE model for the anti-symmetric A_0 and symmetric modes (S_0 and SH_0) respectively. Figs.3(c) and 3(d) show the equivalent results obtained from the asymptotic analytic model. Figs.3(e) and 3(f) show the results from the asymptotic analytic model separated into contributions from the S_0 and SH_0 modes.

It can be seen that the FE and analytical models are in reasonable agreement with regard to the overall pattern of the radiated wave field and its amplitude. Of particular interest here is the behavior of the SH_0 mode. The latter has a highly anisotropic velocity profile and over the range of propagation angles from 6° to 84° has three possible values of

γ_m , resulting in three different wave packets (the third and fastest SH_0 wave packet propagates with a similar profile to the S_0 mode but is of low amplitude and is scarcely visible in the figure). The velocity discrepancy between the models is particularly apparent for the slower SH_0 components around 45° . At the extremities of the angular range where the SH_0 modes exist, it can be seen that there is an abrupt discontinuity in displacements. This represents the breakdown of the asymptotic approximation in (10), since at these points the coefficient b_m in expression (11) is equal to zero and group velocity direction is stationary.

Property	Values						Unit
Density	1560						kg m^{-3}
Stiffness matrix							
$c_{11}, c_{12}, c_{13}, c_{14}, c_{15}, c_{16}$	64.24,	5.6,	7.73,	0,	0,	0	MN mm^{-2}
$c_{21}, c_{22}, c_{23}, c_{24}, c_{25}, c_{26}$	5.6,	70.87,	8.39,	0,	0,	0	MN mm^{-2}
$c_{31}, c_{32}, c_{33}, c_{34}, c_{35}, c_{36}$	7.73,	8.39	13.3	0,	0,	0	MN mm^{-2}
$c_{41}, c_{42}, c_{43}, c_{44}, c_{45}, c_{46}$	0,	0,	0,	2.97,	0,	0	MN mm^{-2}
$c_{51}, c_{52}, c_{53}, c_{54}, c_{55}, c_{56}$	0,	0,	0,	0,	3.06,	0	MN mm^{-2}
$c_{61}, c_{62}, c_{63}, c_{64}, c_{65}, c_{66}$	0,	0,	0,	0,	0,	4.7	MN mm^{-2}

Table 1. Properties of cross-ply composite plate.



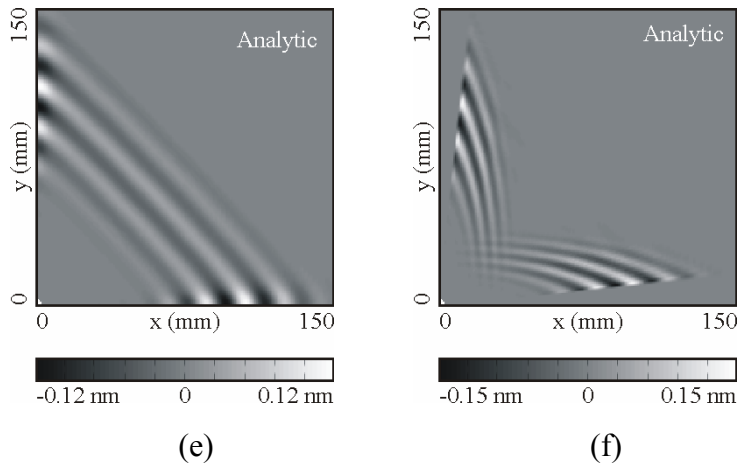


Fig.3. Out-of-plane surface displacement of a cross-ply composite plate: FE model results showing contributions from (a) A_0 mode and (b) $S_0 + SH_0$ modes; analytic model results showing contributions from (c) A_0 , (d) $S_0 + SH_0$ modes, (e) S_0 mode and (f) SH_0 mode.

9. Conclusion

A mathematical basis of a far-field asymptotic analytic technique for predicting the modal amplitude of the 3D guided wave field due to a harmonic point force applied to the surface of a planar multi-layered anisotropic waveguide has been described. The amplitude of the displacement fields of each mode is related to the input force by modal excitability matrices which are functions of direction and frequency. A key attribute of the technique is that the excitability matrices in the 3D case are computed from the excitability matrices for the 2D case of straight crested waves excited by line sources. The latter are readily obtained from modal dispersion data that can be computed by a number of existing methods. The numerical implementation of the technique has been discussed and practical challenges highlighted. Example results from a number of test cases have been presented which show generally good agreement with 3D time-marching finite element simulations. The points where the asymptotic assumptions are invalid are clearly visible in these results and relate to the points where the normal to the phase slowness surface of a mode (i.e. the group velocity direction) is stationary.

In principle a more accurate asymptotic approximation at the vicinity of these points could be obtained but this has not yet been implemented.

References

- [1] M. J. S. Lowe, Matrix techniques for modeling ultrasonic waves in multilayered, IEEE Trans. Ultrason., Ferroelect., Freq. Contr., vol. 42, no. 4, pp. 525-542, 1995.
- [2] T. Hayashi, W.-J. Song and J. L. Rose, Guided wave dispersion curves for a bar with an arbitrary cross-section, a rod and rail example, Ultrasonics, vol. 41, pp. 175-183, 2003.
- [3] B. Pavlakovic, M. Lowe, D. Alleyne and P. Cawley, DISPERSE: A general purpose program for creating dispersion curves, in Review of Progress in Quantitative NDE, edited by D. Thompson and D. Chimenti, vol. 16, pp. 185-192, Plenum, New York, 1997.
- [4] E. Glushkov, N. Glushkova, Blocking property of energy vortices in elastic waveguides, J. Acoust. Soc. Amer., vol. 102, no.3, pp. 1356-1360, 1997.
- [5] M. Veidta, T. Liub and S. Kitipornchai, Modelling of Lamb waves in composite laminated plates excited by interdigital transducers, NDT and E International, vol. 35, pp. 437-447, 2002.

- [6] B. A. Auld, Acoustic fields and waves in solid, 2nd edition, Krieger publishing company, Malabar, 1990.
- [7] V. A. Babeshko, E. V. Glushkov and N. V. Glushkova, Energy vortices and backward fluxes in elastic waveguides, *Wave Motion*, vol. 16, pp. 183-192, 1992.
- [8] A. Mal, Elastic waves from localized sources in composite laminates, *Int. J. Solids and Structures*, vol. 39, pp. 5481-5494, 2002.
- [9] J. D. Achenbach and Y. Xu, Wave motion in an isotropic elastic layer generated by a timeharmonic point load of arbitrary direction, *J. Acoust. Soc. Amer.*, vol. 106, no. 1, pp. 83-90, 1999.
- [10] O. Diligent and M. J. S. Lowe, Reflection of the the S0 Lamb Wave mode from a flat bottom circular hole, *J. Acoust. Soc. Amer.*, vol. 118, no. 5, pp. 2869-2879, 2005.
- [11] D. E. Chimenti, Guided waves in plates and their use in materials characterization, *Appl. Mech. Rev.*, vol. 50, pp. 247-284, 1997.